JOURNAL OF VIROLOGY, Nov. 2000, p. 10571–10580 Vol. 74, No. 22
0022-538X/00/$04.00+0

The Leader RNA of Coronavirus Mouse Hepatitis Virus Contains an Enhancer-Like Element for Subgenomic mRNA Transcription

YICHENG WANG AND XUMING ZHANG*

Department of Microbiology and Immunology, University of Arkansas for Medical Sciences, Little Rock, Arkansas 72205

Received 28 April 2000/Accepted 15 August 2000

While the 5′ *cis*-acting sequence of mouse hepatitis virus (MHV) for genomic RNA replication has been determined in several defective interfering (DI) RNA systems, it remains elusive for subgenomic RNA transcription. Previous studies have shown that the leader RNA in the DI genome significantly enhances the efficiency of DI subgenomic mRNA transcription, indicating that the leader RNA is a *cis*-acting sequence for mRNA transcription. To further characterize the *cis*-acting sequence, we made a series of deletion mutants, all but one of which have an additional deletion of the *cis*-acting signal for replication in the 5′ untranslated region. This deletion effectively eliminated the replication of the DI-chloramphenicol acetyltransferase (CAT)-reporter, as demonstrated by the sensitive reverse transcription (RT)-PCR. The ability of these replication-minus mutants to transcribe subgenomic mRNAs was then assessed using the DI RNA-CAT reporter system. Results from both CAT activity and mRNA transcripts detected by RT-PCR showed that a 5′-proximal sequence of 35 nucleotides (nt) at nt 25 to 59 is a *cis*-acting sequence required for subgenomic RNA transcription, while the consensus repeat sequence of the leader RNA does not have such effect. Analyses of the secondary structure indicate that this 35-nt sequence forms two stem-loops conserved among MHVs. Deletion of this sequence abrogated transcriptional activity and disrupted the predicted stem-loops and overall RNA secondary structure at the 5′ untranslated region, suggesting that the secondary structure formed by this 35-nt sequence may facilitate the downstream consensus sequence accessible for the discontinuous RNA transcription. This may provide a mechanism by which the 5′ *cis*-acting sequence regulates subgenomic RNA transcription. The 5′-most 24 nt are not essential for transcription, while the 9 nt immediately downstream of the leader enhances RNA transcription. The sequence between nt 86 and 135 had little effect on transcription. This study thus defines the *cis*-acting transcription signal at the 5′ end of the DI genome.

Mouse hepatitis virus (MHV) is the prototype of *Murine coronavirus*, a member of the family *Coronaviridae*. MHV contains a positive-sense, single-stranded RNA genome 31 kb long, which encodes seven to eight genes (16, 18, 22). Upon infection, MHV releases its genomic RNA into the cytoplasm, where viral replication and transcription take place. The viral genomic RNA first serves as a messenger RNA for translation of the most-5′-end open reading frame (ORF), the gene 1, which encodes a polyprotein of more than 800 kDa (16). This polyprotein complex contains several proteases and RNA-dependent RNA polymerase activities that are essential for subsequent RNA replication and transcription. The polymerase complex then utilizes the genomic RNA as a template for the synthesis of a genome-length minus-sense RNA, which in turn serves as a template for synthesis of a plus-sense genomic RNA and possibly of six to seven subgenomic mRNAs, all of which share the 5′ and 3′ ends (15, 19; see also reference 16 and references therein). Each subgenomic mRNA contains a leader sequence of approximately 70 nucleotides (nt) at the 5′ end, which is identical to the genomic RNA leader (14, 17, 36). Depending on virus strains, there are two to four UCUAA pentanucleotide repeats, with the last repeat being UCUAA AC, at the 3′ end of the leader (28, 30). An identical UCUA AAC consensus or a similar sequence is present upstream of each gene coding region and is termed the intergenic (IG) sequence (3, 35). Since each subgenomic mRNA starts with a leader RNA fused to a respective IG region, the IG sequence is considered a leader-fusion site for subgenomic RNA transcription.

Based on these unique structural features of the subgenomic mRNAs, several models have been proposed to explain the biogenesis of the subgenomic mRNAs (2, 39; see also reference 16 and references therein). The original leader-primed transcription model proposed that leader RNA is first transcribed from the genome-length, minus-strand RNA, dissociates from the template, and then joins to the downstream IG sequence of the template as a primer to initiate subgenomic mRNA transcription (1, 10, 13–15, 17, 31, 36). An alternative model, i.e., discontinuous transcription during minus-strand RNA synthesis, was also proposed based on the findings that subgenomic replicative intermediates and subgenomic minus-strands complementary to each subgenomic mRNA were present in coronavirus-infected cells (33, 34). Recently, it has been shown that the subgenomic minus-strand RNAs are functional templates for mRNA synthesis (2). Either model is compatible with some but not all experimental data, but the models are not necessarily mutually exclusive; they may be operative at different stages during the virus replication cycle. The precise mechanism of coronavirus subgenomic mRNA transcription thus remains elusive.

The *cis*-acting sequences for coronavirus genomic RNA replication have been determined in several defective interfering (DI) RNA systems (5, 11, 12, 23, 26). The sequences required for MHV genomic RNA replication consist of 470 to 859 nt from the 5′ end and 436 nt from the 3′ end of the genome (11, 12, 23). An additional 135-nt internal sequence located at gene

* Corresponding author. Mailing address: Department of Microbiology and Immunology, University of Arkansas for Medical Sciences, 4301 W. Markham St., Slot 511, Little Rock, AR 72205. Phone: (501) 686-7415. Fax: (501) 686-5359. E-mail: zhangxuming@exchange.uams.edu.

1 was found to be required for replication of DI RNA derived from JHM (11, 12, 23). For minus-strand RNA synthesis, only a 55-nt sequence plus the poly(A) tail at the 3′ end of the genome is sufficient (24). The major *cis*-acting sequence for subgenomic mRNA transcription is apparently the IG sequence, since the insertion of an IG sequence into a DI RNA facilitates the synthesis of a subgenomic mRNA from that IG site (27). Furthermore, it has been shown that the 3′ end 270 nt is also required for subgenomic mRNA transcription from a reporter DI RNA (25). We and others previously showed that the leader RNA has both *cis*- and *trans*-acting activities on subgenomic mRNA transcription from a reporter DI RNA (22, 44). The leader RNA derived in *trans* and, under certain circumstances, also in *cis* (i.e., from a different or the same RNA molecule) is incorporated into subgenomic mRNAs (10, 44). Deletion of the leader sequence from an RNA template resulted in significant loss of transcription activity, even though the leader RNA for subgenomic mRNA could have been provided in *trans* by the helper virus (22). In addition, we have demonstrated that a 9-nt sequence immediately downstream of the leader can upregulate the efficiency of subgenomic mRNA transcription (42, 43). These findings suggest that MHV subgenomic mRNA transcription requires an IG sequence and a 270-nt at the 3′ end and is regulated by a *cis*-acting sequence at the 5′ end and a *trans*-acting leader RNA.

The precise *cis*-acting sequence at the 5′ end of MHV genomic RNA for subgenomic mRNA transcription is not known. In the present study, we have employed the DI RNA-reporter system to systematically dissect the 5′-end *cis*-acting sequence for subgenomic mRNA transcription. Results from the present study are in general agreement with our previous findings, i.e., the *cis*-acting leader RNA as a whole up-regulated subgenomic mRNA transcription. Surprisingly, however, when the leader RNA was further delineated, we found that the up-regulatory element resides within the 5′-proximal 35 nt of the leader while the downstream UCUAA repeat sequence does not support transcription. The consensus repeats even down-regulate subgenomic mRNA transcription to some extent. Secondary-structure analysis indicates that the 35-nt sequence forms two stem-loops, which may allow the downstream UCUAAAC to be accessible during the discontinuous transcription process. This may provide a mechanism by which the 5′ *cis*-acting sequence regulates subgenomic RNA transcription.

MATERIALS AND METHODS

Viruses and cells. MHV JHM(2) was used as a helper virus for infection (29). The murine astrocytoma cell line DBT (8) was used for virus propagation, virus infection, and RNA transfection experiments throughout this study.

Plasmid construction. A previously described DI RNA-chloramphenicol acetyltransferase (CAT) reporter plasmid, pDE-CAT2-1(3), which contains the 5′ end sequence of JHM(3) and the CAT gene under the control of the IG sequence for mRNA2-1 (IG2-1) (see Fig. 2A) (43), was used as a basic plasmid for construction of most deletion plasmids. For construction of DI reporter plasmids containing deletions downstream of the leader RNA, a separate DI cloning vector was generated. pDECAT2-1(3) DNA was used as a template for PCR to amplify the 5′-end sequence of the leader with the primer M13-20 (5′-GTA AAA CGA CGG CCA GT-3′), which corresponds to a sequence upstream of the T7 promoter in the vector pBluescript (Stratagene), and the primer 3′StuL57 (5′-*ATA GGC CT*A AAC TAC AAG AGT-3′), which is complementary to nt 44 to 57 of the leader and contains a *Stu*I site (underlined) at the 5′ end. Note that extra sequences in a primer (not represented by DI sequences) are indicated by italic throughout this section. PCR was performed at 95°C for 30 s, 56°C for 1 min, and 72°C for 2 min in a PCR buffer (20 mM Tris [pH 8.3], 25 mM KCl, 1.5 mM $MgCl_2$, 0.1% Tween 20, a 200 μM concentration of each nucleoside triphosphate, 20 pmol of each primer) for 25 cycles. The same PCR condition was used for all plasmid DNA constructions. The PCR fragment was digested with *Sna*BI (at nt 24 of the leader) and *Stu*I, and was cloned into the *Sna*BI and *Stu*I sites of pDECAT2-1(3) vector. The orientation of the inserts was confirmed by further restriction enzyme analyses. Since the natural *Stu*I site is located at nt 486 of pDECAT2-1(3) vector, the resultant plasmid pDECAT2-1Δ60-486 has deleted a sequence from nt 60 to 486 of the DI genome and replaced the two nucleotides (AA) at nt 58 to 59 of pDECAT2-1 with GG due to the creation of the *Stu*I site. For making pLΔ60-85, pLΔ60-95, pLΔ60-105, pLΔ60-115, and pLΔ60-135, PCR fragments were generated from pDECAT2-1(3) DNA template using the 5′ primer 5′-UTR86 (5′-GGC ACT TCC TGC GTG TCC-3′, corresponding to nt 86 to 103 of the DI genome), 5′-UTR96 (5′-GCG TGT CCA TGC CCG TGG-3′, corresponding to nt 96 to 113), 5′-UTR106 (5′-GCC CGT GGG CCT GGT CTT-3′, corresponding to nt 106 to 123), 5′-UTR116 (5′-CTG GTC TTG TCA TAG TGC-3′, corresponding to nt 116 to 133), or 5′-UTR136 (5′-ACA TTT GTG GTT CCT TGA-3′, corresponding to nt 136 to 153), respectively, and the 3′ primer 3′A499 (5′-CAT CAT AGT CGA GGC CTC CAC-3′, complementary to nt 479 to 499 of the DI genome with a natural *Stu*I site at nt 486). PCR fragments were blunt ended with T4 DNA polymerase at the 5′ end, digested with *Stu*I at the 3′ end, and cloned into the *Stu*I site of pDECAT2-1Δ60-486, generating pLΔ60-85, pLΔ60-95, pLΔ60-105, pLΔ60-115, and pLΔ60-135, which has deleted a sequence from nt 60 to 85, nt 60 to 95, nt 60 to 105, nt 60 to 115, and nt 60 to 135, respectively (see Fig. 2B). pL2R9nt and pL1R were constructed in the same way using the 5′ primer 5′2R9ntUTR116 (5′-TCT AAT CTA AAC TTT ATA AAC CTG GTC TTG TCA TAG-3′, containing two repeats and the 9-nt sequence at the 5′ end and a 15-nt sequence at nt 116 to 130), and 5′1RUTR116 (5′-TCT AAA CCT GGT CTT GTC ATA GTG-3′, containing one consensus sequence and a 17-nt sequence at nt 116 to 132), respectively, and the 3′ primer 3′A499 in the PCR. All these constructs contain two Gs instead of two As at nt 58 to 59 of the original DI genome.

For constructing pL4R, pL2Rsp, and pL2R, a jumping PCR was carried out. In the first PCR, the 5′-end sequence of the leader was amplified using the 5′ primer M13-20 and the 3′ primer 3′4RUTR116 (5′-CTA TGA CAA GAC CAG GTT TAG ATT AGA TTA GAT TAG ATT TAA-3′, containing four repeats [underlined], a 5-nt sequence at the 3′ end complementary to nt 55 to 59, and 15 nt at the 5′ end complementary to nt 116 to 130), 3′2RspUTR116 (5′-CTA TGA CAA GAC CAG *GTT ACA CCA* GTT TAG ATT AGA TTT AA-3′, containing the same sequence as 3′4RUTR116 except for the two repeats [underlined] and a nonspecific 9-nt sequence [italic] in place of the four repeats), and 3′2RUTR116 (5′-CTA TGA CAA GAC CAG GTT TAG ATT AGA TTT AA-3′, containing the same sequence as 3′4RUTR116 except for the two repeats [underlined] in place of the four repeats), respectively. Plasmid DNA pDECAT2-1(2) (44) was used for primers 3′2RUTR116 and 3′2RspUTR116, and p25CAT was used (22) for 3′4RUTR116. In the second PCR, a fragment downstream of the leader was amplified using the same DNA template but a different primer pair, 5′UTR116 and 3′A499, as described above. Products from the two PCR amplifications were purified by agarose gel electrophoresis with the gel elution kit (QIAGEN Inc.). The two fragments from the first and the second PCR were then mixed in the third (jumping) PCR using the primer pair M13-20 and 3′A499. PCR products from the third PCR were digested with *Sna*BI (at nt 24) and *Stu*I (at nt 486) and directionally cloned into the *Sna*BI and *Stu*I sites of pDECAT2-1(3), generating pL4R, pL2Rsp, and pL2R, respectively. Since both *Sna*BI and *Stu*I generate blunt ends, the orientation of the inserts was verified by both restriction enzyme digestion and PCR reamplification with different pairs of primers.

For generating pLΔ1-115 and p2R9ntΔL59, PCR fragments were synthesized from pDECAT2-1(3) DNA template with the primer pairs 5′UTR116-3′A499 and 5′2R9ntUTR116-3′A499, respectively. PCR products were blunt-ended and digested with *Stu*I and cloned into the *Hin*dIII (blunt ended) and *Stu*I sites of pDECAT2-1(3) vector, generating pLΔ1-115 and p2R9ntΔL59. For making pL25-59, pLΔ60-115 DNA was digested with *Sna*BI (at nt 24) and an upstream *Hin*dIII site, blunt ended with T4 DNA polymerase, and self-ligated, resulting in a deletion of the first 24 nt. pL24 was constructed in the following two steps: a PCR fragment was amplified from pLΔ60-115 DNA template using the primer pair 5′URT116-3′A499, digested with *Stu*I, and blunt-ended with T4 DNA polymerase; pLΔ60-115 DNA was digested with *Sna*BI and *Stu*I, and the smaller *Sna*BI-*Stu*I fragment of pLΔ60-115 was replaced with the PCR fragment (from nt 116 to 486) by ligation.

For constructing pDECAT-350, pDECAT2-1(3) DNA was digested with *Pst*I, which is located immediately downstream of the CAT gene, blunt ended with T4 DNA polymerase, and then digested with *Xba*I. The larger *Pst*I-*Xba*I fragment was isolated from agarose gel following electrophoresis and was used as a vector, which has a deletion of the 3′-end 700-nt *Pst*I-*Xba*I fragment. A 350-nt fragment was excised from pDF-350CAT (25) by digesting the DNA with *Acc*I, blunt ending with T4 DNA polymerase, and then digesting with *Xba*I. This *Acc*I (blunt-end)-*Xba*I fragment (350-nt), which represents the 3′ end of the DI RNA, was cloned into the *Pst*I (blunt-end)-*Xba*I sites of pDECAT2-1(3). The resultant pDECAT-350 thus contains only 350 nt and the poly(A) tail at the 3′ untranslated region.

In vitro RNA transcription and RNA transfection. All plasmid DNAs were linearized with *Xba*I, and the genomic DI RNAs were transcribed in vitro with T7 RNA polymerase as described previously (44). Each in vitro-transcribed RNA sample was quantified by determining the optical density using a spectrophotometer (Beckman) and by agarose gel electrophoresis analysis. Approximately equal amounts of RNAs for each construct were used for transfection. RNA transfection was carried out with the DOTAP {*N*-[1(2,3-dioleoyloxy)propyl]-*N*,*N*,*N*-trimethylammoniumethyl sulfate} method according to the manufacturer's instruction (Boehringer Mannheim) as described previously (44). Briefly,

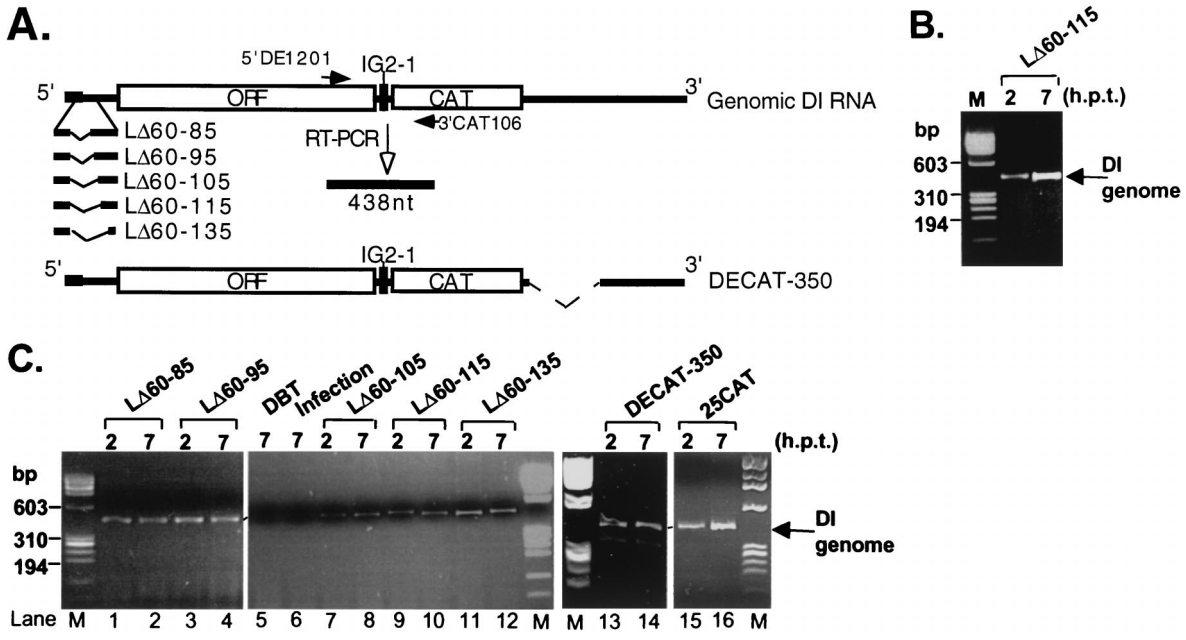

FIG. 1. Generation of replication-minus defective interfering RNA mutants. (A) Schematic diagram of the DI RNA-CAT reporter constructs. The structures of all mutants are identical except for a deletion of various lengths between nt 60 and 135 as indicated. DECAT-350 contains a wild-type leader and the 5′-UTR but has deleted a sequence between the CAT gene and 350 nt upstream from the 3′ end. The DI ORF and the CAT ORF are shown. Two primers used for RT-PCR are indicated with arrows, and the size of the expected RT-PCR product is also shown. IG2-1, IG sequence for subgenomic mRNA2-1 transcription. (B and C), RT-PCR results analyzed by agarose gel electrophoresis. (B) The RNA-transfection mixture remained in the culture throughout. (C) The RNA-transfection mixtures were removed from the culture at 2 h posttransfection (h.p.t.). RNAs were isolated either at 2 or 7 h.p.t. from cells transfected with various DI RNA constructs (shown at the top). Molecular markers are shown on the left, and the RT-PCR products representing DI genome are indicated with an arrow on the right. Lane DBT, DBT cells alone without infection and transfection. Lane Infection, virus-infection alone.

DBT cells were infected with helper virus JHM(2) at a multiplicity of infection of 5 to 10. At 1 h postinfection, cells were transfected with the in vitro-transcribed RNA using the DOTAP transfection reagent. Cells were incubated for a period of time as indicated. Cell lysates were then extracted for determining the CAT activity by the CAT assay as described below. Intracellular RNAs were isolated with the TriZol reagent according the manufacturer's instruction (Life Science Technologies, Inc.) and were used for determining the RNA transcripts by reverse transcription (RT)-PCR (see below).

CAT assay. For the CAT assay, cell lysates were extracted at 7 h posttransfection. The CAT assay was performed as described previously (44).

RT-PCR. For detection of DI-specific RNA in transfected cells, RT-PCR was performed. At an indicated time point after transfection, total intracellular RNAs were isolated with the TriZol reagent (Life Science Technologies, Inc.). cDNAs representing DI RNAs were synthesized by RT using the 3′ primer 3′CAT106 (5′-TCT GGT TAT AGG TAC ATT GA-3′, complementary to a sequence of the CAT gene at nt 87 to 106) or 3′CAT344 (5′-TGC CGG AAA TCG TCG TGG TA-3′, complementary to a sequence of the CAT gene at nt 320 to 340). The RT reaction was carried out at 42°C for 90 min as described previously (44). cDNAs were then amplified by PCR using an additional primer, 5′L9 (5′-TGA TTG GCG TCC GTA CGT ACC-3′, corresponding to MHV leader sequence at nt 9 to 29) or 5′DE1201 (5′-ATC TTA AGT GAG CTT CAA ACC GAA-3′, corresponding to the DI genome at nt 1201 to 1224). The primer pair 5′DE1201-3′CAT106 would amplify the DI genomic RNA with a size of 438 nt; the primer pair 5′L9-3′CAT344 would amplify the subgenomic mRNA with a size of 436 nt. The primer pair 5′DE1201-3′CAT344 amplifies a 676-nt fragment representing the genomic DI RNA. PCR was performed for a total of 20 cycles in a thermocycler (DNA Engine; M.J. Research Inc.) with each cycle at 95°C for 1 min for denaturation, 60°C for 1 min for annealing, and 72°C for 1 min for extension. RT-PCR products were analyzed by agarose gel electrophoresis, stained with ethidium bromide, and photographed with a gel document apparatus (Stratagene). Images were saved as a TIFF file and labeled using PowerPoint software (version 4.0).

For detection of minus-strand DI RNA, the RT-PCR procedure described above was slightly modified. Briefly, in the RT reaction, the sense primer 5′CAT (5′-ATG GAG AAA AAA AT-3′, corresponding to the first 14 nt of the CAT gene) was used. In the first round of PCR, the primer pair 5′CAT and 3′CAT542 (5′-TTA CGC CCC GCC CTG CCA CTC ATC GC-3′, complementary to the 3′-end of the CAT gene) was used, and PCR was performed for 30 cycles. PCR products were reamplified in a second-round PCR for 30 cycles with the primer pair 5′CAT and 3′CAT344. PCR products from the second round represent the minus-strand DI RNA with a size of 344 nt.

RESULTS

Characterization of the 5′ *cis*-acting sequence for subgenomic mRNA transcription. A previously developed DI RNA-CAT reporter system (22, 44) was used for dissecting the 5′-end *cis*-acting sequence for subgenomic mRNA transcription. In this system, the CAT gene is inserted into an MHV DI RNA under the control of an MHV IG sequence (Fig. 1A). Transfection of the genomic DI RNA transcribed in vitro by T7 RNA polymerase into helper MHV-infected cells results in the expression of the CAT activity. Since the CAT gene is placed in the second ORF in the DI, the CAT activity cannot be expressed from the bicistronic DI genomic RNA (22). Therefore, the expression of the CAT activity completely depends on the transcription of a subgenomic CAT mRNA from the IG site of the genomic DI RNA. It was previously assessed that the CAT activity quantitatively reflected the efficiency of subgenomic mRNA transcription in this system (22). However, it is conceivable that, if the efficiency of DI genomic RNA replication is altered due to mutations in the *cis*-acting replication signal as in the case of this study, the CAT activity could not faithfully reflect the efficiency of subgenomic mRNA transcription. For example, if both the primary transfected DI RNA and the secondary replicated DI RNA are to be used for subgenomic DI RNA transcription, a DI RNA with a deletion in the 5′-*cis*-acting replication signal would result in reduced synthesis of subgenomic mRNAs due to a lack of supply of replicated DI genomic RNA templates, even though the efficiency of subgenomic mRNA from a given amount of the templates remains unchanged. To unequivocally determine the 5′-end *cis*-acting sequence for subgenomic mRNA transcription, it is thus essential to eliminate the replication signal. However, this would pose a problem if both replication and transcription

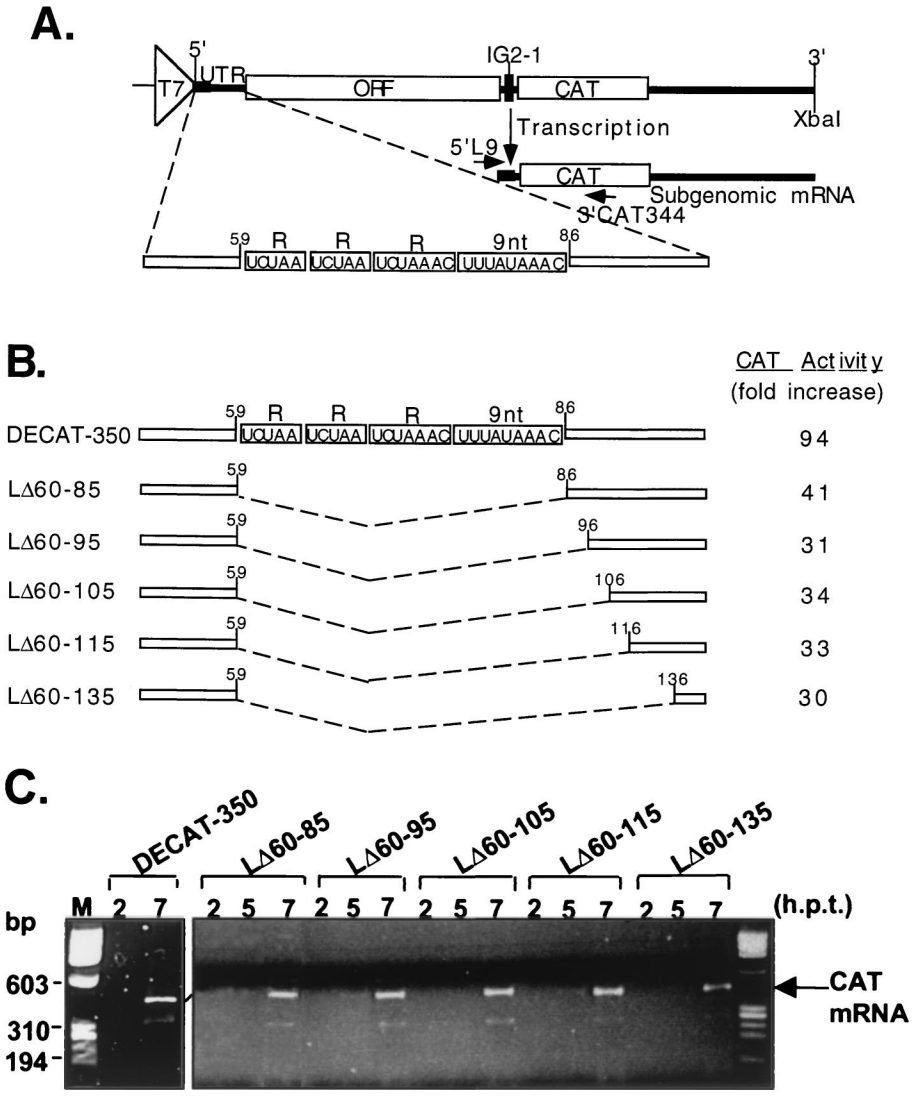

FIG. 2. Deletion analysis of the *cis*-acting sequence at the 5′-UTR for subgenomic mRNA transcription. (A) Schematic diagram of the DI RNA-CAT reporter system. The DI ORF, the CAT ORF, the IG sequence for subgenomic mRNA transcription, the T7 promoter for in vitro transcription, the *Xba*I restriction site, the 5′-UTR, and primers used for RT-PCR are indicated. The numbers indicate the nucleotide position from the 5′ end of the viral genome. R, consensus repeat. (B) Results of CAT analysis. The names, structures and CAT activities are shown from left to right. The activities are the averages of three independent experiments and are indicated as fold increase against the background, which is set as 1. (C) RT-PCR results analyzed by agarose gel electrophoresis. The time when RNAs were isolated is indicated as hours posttransfection (h.p.t.) at the top. Transfected DI RNA constructs are also shown at the top. Molecular markers (lane M) are shown on the left, and the RT-PCR products representing DI CAT subgenomic mRNA are indicated with an arrow on the right.

signals are the same or largely overlapping at the 5′ end of the genome. The finding that a replication-minus DI construct, LStu480, which contains the leader RNA but has deleted the most-5′ *cis*-acting replication signal, was still capable of transcribing subgenomic mRNA (22) allowed us to make various replication-minus DI-CAT reporter vectors and to determine their abilities in transcribing subgenomic mRNAs.

Previously, Kim and Makino (11) reported that two DI constructs, which deleted 21 nt (from nt 56 to 87) and 78 nt (from nt 87 to 165), respectively, did not replicate in MHV-infected cells; genomic DI RNAs were not detected by Northern blot analysis. Based on that information, we made five DI RNA-CAT constructs, all of which have an additional deletion from nt 56 to 85 (Fig. 1 and 2). In addition, Lin et al. (25) reported that a DI reporter construct, DF-350CAT, which contains 350 nt plus the poly(A) tail at the 3′ end, was capable of transcribing subgenomic CAT mRNA but was unable to replicate. Since DF-350CAT contains the intact leader RNA, we made a new construct, DECAT-350, whose 3′ end contains the 350 nt derived from DF-350CAT (Fig. 1A). This construct was used as a control for replication-deficient and transcription-competent DI RNA. To ensure that these deletion constructs are indeed not replication competent, we employed a more-sensitive method, RT-PCR, in an attempt to detect low levels of RNA transcripts, which might have escaped from the Northern blot detection previously (11). Cells were infected with MHV JHM(2) and transfected with in vitro-transcribed DI genomic RNAs from these constructs. Results showed that when the RNA-transfection reagent mixture remained in the cell culture throughout the 7-h transfection period, increased levels of DI genomic RNAs were detected from 2 to 7 h posttransfection (an example is shown in Fig. 1B; further data not shown). This suggests that DI RNAs were either continuously delivered (by transfection) into cells or replicated (from transfected RNA) from 2 to

7 h posttransfection. To distinguish these two possibilities, the transfection mixture was removed and replaced with fresh medium at 2 h posttransfection. RNAs were isolated at 7 h posttransfection and subjected to RT-PCR detection. This treatment would effectively eliminate the detection of any increased amount of DI genomic RNAs if it was due to continuous RNA transfection, and it would not, if the increase was caused by RNA replication. As shown in Fig. 1C, no increase of genomic DI RNAs was detected in deletion mutants-transfected cells from 2 to 7 h posttransfection (lanes 1 to 4 and 7 to 14), while the amount of genomic RNA from the replicating, wild-type DI-CAT reporter (25CAT) was significantly increased (compare lane 15 with lane 16), indicating that all deletion constructs are indeed not replication competent. These RNAs are DI-specific because neither cellular RNAs nor viral RNAs were detected with the same primer pair in RT-PCR (Fig. 1C, lanes 5 and 6).

Next, the effect of the 5′ *cis*-acting sequence on subgenomic mRNA transcription was examined. Since the above experiments showed that these DI constructs are not replicative, any detection of subgenomic mRNAs from these deletion constructs would be indicative of transcription from primary transfected DI RNAs. Cells were infected with JHM(2) and transfected with in vitro-transcribed DI RNAs. Cell lysates were extracted at 6 h posttransfection for CAT assay or total RNAs were isolated at various time points for RT-PCR for detection of subgenomic CAT-containing DI RNAs (Fig. 2A). As shown in Fig. 2B, systematic deletions from nt 95 to 135 of the 5′ sequence did not significantly affect the CAT activities. A deletion from nt 60 to 85 resulted in a reduction of the CAT activity by approximately twofold (compare DECAT-350 and LΔ60-85). CAT activity expressed from LΔ60-85 was approximately 24% higher than those from downstream deletion mutants (e.g., compare LΔ60-85 with LΔ60-115). These results indicate that the sequence between nt 60 and 85, and to a less extent, the sequence between nt 86 and 95 of the 5′ untranslated region (5′-UTR) enhance the reporter gene expression. To confirm that CAT-containing subgenomic mRNAs are transcribed from these constructs, RT-PCR was performed with CAT-specific primers. While the RT-PCR was not quantitative, results showed that a 436-nt PCR product, which represents the CAT-containing subgenomic mRNAs, was detected in all deletion constructs (Fig. 2C). The identity of the CAT-containing subgenomic mRNAs was further confirmed by sequencing the RT-PCR products for LΔ60-115 (data not shown). The origin of the smaller band was not determined (Fig. 2C). Taken together, we conclude that the sequence between nt 60 and 95 enhances subgenomic mRNA transcription, whereas the downstream sequence (between nt 96 and 135) has no such effect.

Identification of an enhancer-like element within the leader RNA for subgenomic mRNA transcription. It has been demonstrated previously that the leader RNA has an enhancer-like activity in subgenomic mRNA transcription (22) and that the 9-nt sequence immediately downstream of the leader up-regulates mRNA transcription (42, 43). However, whether these 5′ sequences are required or are merely auxiliary enhancer-like sequences for mRNA transcription has not been determined. Also not known is whether the complete or part of the leader RNA constitutes this enhancer-like activity. We initially speculated that the consensus repeats along with the 9-nt sequence might be the enhancer-like element, since these sequences are important for both leader-IG sequence fusion and leader switching (29). To test this hypothesis, we made four DI RNA-CAT reporter constructs containing or lacking the consensus repeats and the 9-nt sequence, all of which were not replicative as confirmed by RT-PCR (Fig. 3C, further data not shown). Contrary to our expectation, the result showed that deletion of the 5′-end 59-nt sequence (construct 2R9ntΔL59) completely abolished the CAT activity, a result similar to that of LΔ1-115, whose entire leader is deleted (Fig. 3A). Addition of the 5′-end 59-nt sequence significantly enhanced the CAT activity (construct LΔ60-115 in Fig. 3A). More surprisingly, addition of two consensus repeats decreased the CAT activity by approximately sixfold (compare construct L2R with LΔ60-115 in Fig. 3A). These results were reproducible in more than 10 separate transfection experiments. We thus conclude that the 5′-end 59-nt sequence is a *cis*-acting sequence consisting of an enhancer-like element.

To confirm that the CAT activities detected reflect the efficiency of subgenomic mRNA transcription, we performed RT-PCR to directly detect subgenomic CAT-containing mRNAs in MHV-infected and DI RNA-transfected cells. We used the CAT-specific primer 3′CAT344 in the RT reaction and a leader RNA-specific primer in PCR. This primer pair would detect the subgenomic DI RNAs of 436 nt in length (Fig. 2A). As shown in Fig. 3B, subgenomic RNA was detected strongly in LΔ60-116 RNA-transfected cells but weakly in L2R RNA-transfected cells. No subgenomic RNA was detected in LΔ1-115- and 2R9ntΔL59-RNA-transfected cells, even after 10 cycles of further amplification (data not shown). In the control experiments, no CAT-containing subgenomic DI RNA was detected in RNA samples isolated from MHV-infected and mock-transfected cells or in samples mixed with genomic DI RNAs transcribed in vitro (Fig. 3B, lanes Mock Tx and IVT). To exclude the possibility that the failure of detection of subgenomic mRNA was not due to an insufficient transfection of DI RNAs, RT-PCR was carried out to determine the presence of genomic DI RNA. As shown in Fig. 3C, genomic DI RNAs were detected from all RNA samples isolated from various DI-transfected, but not from mock-transfected cells at 7 h posttransfection. Minus-strand DI RNAs were also detected in these deletion mutants-transfected cells (Fig. 3D), indicating that the 5′-end sequence does not affect minus-strand RNA synthesis. This result is consistent with the finding of Lin et al. (24) that a sequence of 50 nt plus the poly(A) tail at the 3′-end is sufficient for minus-strand RNA synthesis.

The sequence between nt 25 and 59 of the leader is the core enhancer-like element. To further dissect the enhancer-like element within the first 59 nt of the leader, we made two additional deletion constructs. L25-59 deleted the 5′-end 24-nt, while L24 deleted a sequence from nt 25 to 115. As shown in Fig. 4A, the CAT activity from L25-59 (36-fold increase) was comparable to that from LΔ60-115 (33-fold increase), whereas the CAT activity from L24 was significantly reduced to 1.6-fold above the background level. Consistent with the CAT activities, RT-PCR detected CAT-containing subgenomic mRNAs in LΔ60-115- and L25-59-transfected cells but not in L24-transfected cells at 7 h posttransfection. To ensure that relatively similar amounts of DI RNAs were transfected into cells, RT-PCR was used to detect the genomic DI RNA at 7 h posttransfection. The intensities of the PCR bands were similar among various deletion constructs (Fig. 4C), although it was not a quantitative PCR. Consistent with this finding is the detection of minus-strand DI RNA in all constructs (Fig. 4D). Taken together, these results indicate that the enhancer-like element mainly resides within the 35-nt sequence between nt 25 and 59 of the leader RNA.

The consensus repeats of the leader do not possess an enhancer-like activity for subgenomic RNA transcription. To further dissect the leader RNA, we made three additional constructs containing one, two, and four consensus repeats,

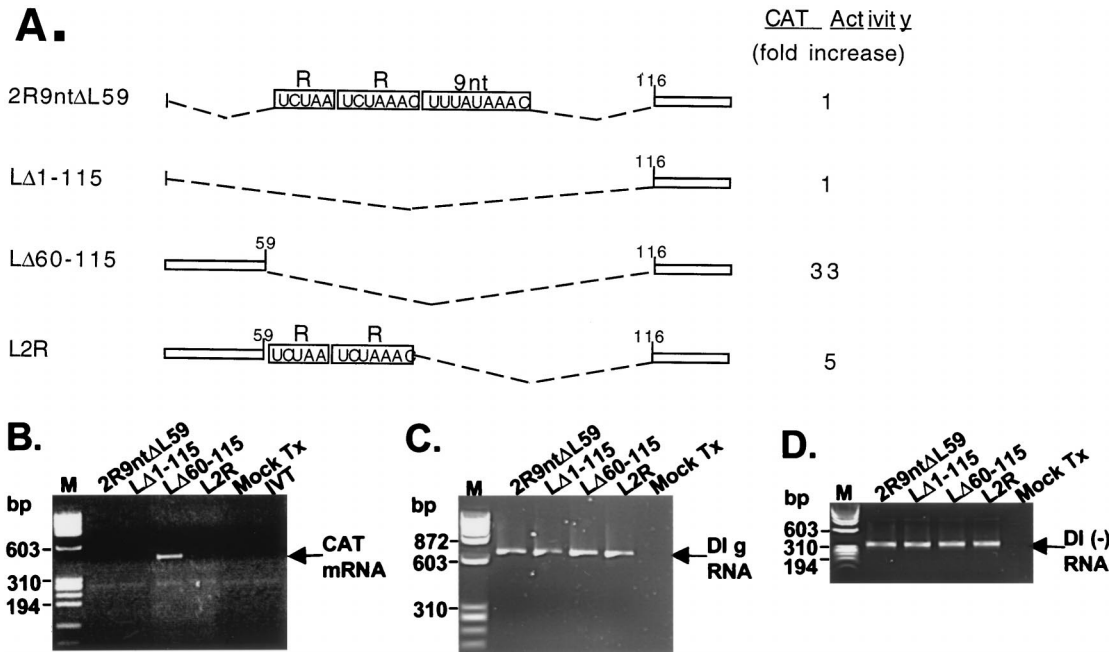

FIG. 3. Dissection of the leader sequence for subgenomic RNA transcription. (A) Results of the transcriptional analysis. The names, structures (only the 5′-end regions are shown; the remaining part is the same as in Fig. 2A), and CAT activities are shown from left to right. The CAT activities are the averages of three independent experiments and are indicated as fold increase against the background, which is set as 1. (B to D) RT-PCR results analyzed by agarose gel electrophoresis. Transfected DI RNAs are shown at the top. All RNA samples were isolated at 7 h posttransfection. IVT, a negative control, in which RNAs transcribed from in vitro transcription were used directly for RT-PCR. Molecular markers (lane M) are shown on the left, and the RT-PCR products representing DI subgenomic mRNA (B), DI genomic RNA (C), and DI minus-strand RNA (D) are indicated with an arrow to the right of each panel. Mock Tx, a negative control, in which RNAs were isolated from helper virus-infected and mock-transfected cells.

respectively. As shown in Fig. 5, the CAT activities from these constructs were approximately three to six times reduced (constructs L1R, L2R, and L4R), compared with that from construct LΔ60-115, which lacks any consensus repeats. Addition of the 9-nt sequence downstream of the two repeats increased the CAT activity by sixfold (construct L2R9nt), indicating that the 9-nt sequence up-regulates mRNA transcription. To determine whether this enhancing activity is sequence-specific for

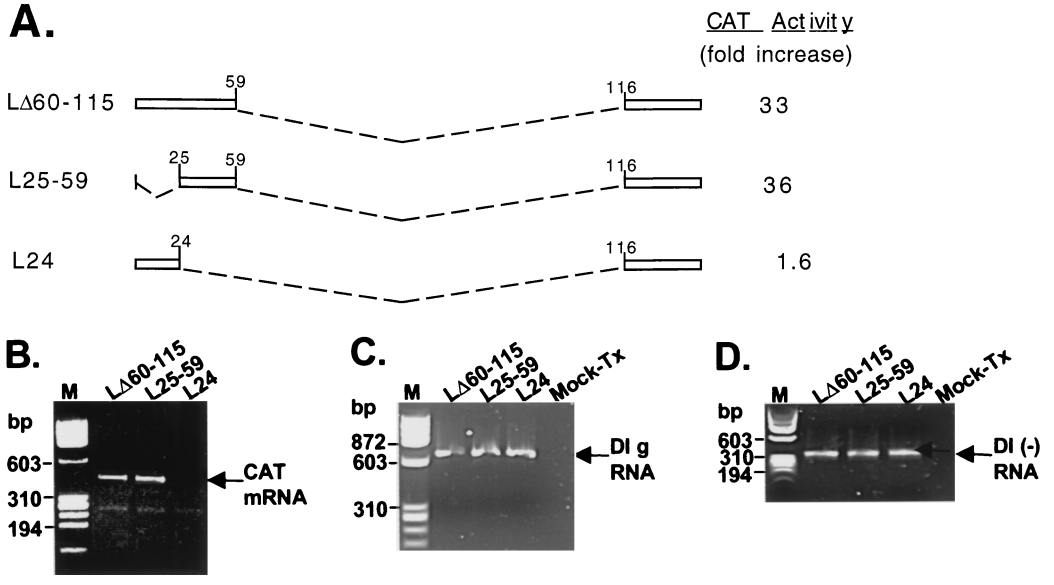

FIG. 4. Mapping of the enhancer-like element for subgenomic mRNA transcription. (A) Results of the transcriptional analysis. The names, structures (only the 5′-end regions are shown; the remaining part is the same as in Fig. 2A), and CAT activities are shown from left to right. The CAT activities are the averages of three independent experiments and are indicated as fold increase against the background, which is set as 1. (B to D), RT-PCR results analyzed by agarose gel electrophoresis. Transfected DI RNAs are shown at the top. All RNA samples were isolated at 7 h posttransfection. Molecular markers (lane M) are shown on the left, and the RT-PCR products representing DI subgenomic mRNA (B), DI genomic RNA (C), and DI minus-strand RNA (D) are indicated with an arrow to the right of each panel. Mock Tx, a negative control, in which RNAs were isolated from helper virus-infected and mock-transfected cells.

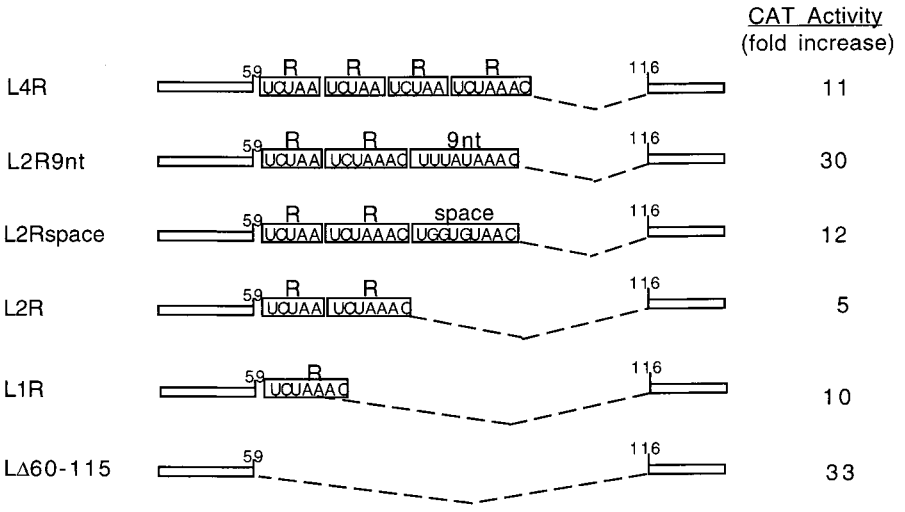

FIG. 5. Fine mapping of the consensus sequence of the leader RNA for subgenomic mRNA transcription. The names, structures (only the 5′-end regions are shown; the remaining part is the same as in Fig. 2A), and CAT activities are shown from left to right. The CAT activities are the averages of three independent experiments and are indicated as fold increase against the background, which is set as 1. R, consensus repeat sequence; space, a spacer sequence.

the 9 nt, we used the computer programs Mfold (45) and LoopDloop (D. G. Gilbert, 1992, published electronically at ftp.bio.indiana.edu) to analyze the secondary structure of the 5′-UTR of MHV RNA. Based on the computer-predicted secondary structure, the 9 nt (UUUAUAAAC) was replaced with a sequence containing the same number of nucleotides (UGG UGUAAC) and the same secondary structure (data not shown). Transfection of this mutant construct (L2Rspace) into helper virus-infected cells resulted in a decrease of CAT activity by approximately threefold. This suggests that the RNA secondary structure and space in this context do not play a role in regulating transcriptional activity and that the enhancing activity is specific for the 9-nt sequence. This result is in agreement with our previous observation that the 9-nt sequence can up-regulate mRNA transcription (43, 44). We conclude from these results that the consensus repeats of the leader do not possess an enhancer-like activity for subgenomic mRNA transcription and that the 9-nt sequence downstream of the leader specifically enhances subgenomic mRNA transcription in a sequence-specific manner.

DISCUSSION

cis-acting sequences are critical elements for replication and maintenance of population for almost all RNA viruses. They are evolutionarily conserved among certain virus groups. Most, if not all, *cis*-acting sequences reside at both ends of the viral RNA genome. In coronavirus, two classes of *cis*-acting sequences have been identified previously (5, 11, 12, 23, 26). One class is for genomic replication, and the other is for subgenomic RNA transcription. The intergenic sequences at various locations inside the genome are not required for genomic RNA replication but are absolutely required for subgenomic RNA transcription (27). To date, while the *cis*-acting sequence at the 3′ end of the genome has been characterized, the 5′-end sequence for subgenomic RNA transcription has not been well defined, partly due to the complexity of the 5′-end sequence. It has been shown that the 5′ sequence plays a role in genomic replication and subgenomic transcription as well as in translation (11, 22, 23, 26, 38, 44). Also known is that the *trans*-acting leader from the helper virus can affect the DI subgenomic RNA transcription (44). However, what sequence at the 5′ end of the genome is required for subgenomic mRNA transcription is not known, even though the *trans*-leader RNA can prime transcription. In the present study, we have systematically characterized the *cis*-acting sequence at the 5′ end of the coronavirus genome for subgenomic RNA transcription. Our experimental approach was to separate the two RNA synthetic processes (replication and transcription) by making replication-minus mutants. This approach allows us to dissect the *cis*-acting sequence for transcription in the absence of DI genome replication. This is evidenced by the finding that the 5′-end 24-nt sequence of the leader is not required for subgenomic RNA transcription (Fig. 4), whereas this sequence is essential for genomic RNA replication (11, 23). Thus, the 5′ *cis*-acting sequences for genomic replication and subgenomic transcription are separable. This finding also reinforces the notion that in the absence of genomic RNA replication, subgenomic RNA transcription is still active as long as the genomic RNA delivered via transfection is a functional template for subgenomic transcription. This does not suggest, however, that the template for subgenomic transcription has to be the positive-strand genome, since minus-strand RNA synthesis can occur when the 3′-end 50 nt and the poly(A) tail are present (24), which is the case for all DI constructs used in this study (Fig. 3D and 4D).

Interestingly, our results show that the enhancer-like element resides within a 35-nt sequence (between nt 25 and 59) of the leader (Fig. 4). This finding is surprising because we previously assumed that the consensus repeat sequence at the 3′ end of the leader would have such a function. The consensus repeats provide a sequence for leader-mRNA fusion, leader switching, or recombination (28–31) and for interacting with a number of cellular and viral proteins (6, 37). How the 35-nt sequence up-regulates coronavirus RNA transcription remains to be investigated. One possibility is that the 35-nt sequence may interact with viral and cellular proteins of the coronavirus transcription complex, thus acting directly or indirectly through other proteins to up-regulate the transcription. This finding leads us to reexamine whether this sequence interacts with those cellular proteins that have been identified (such as heterogeneous nuclear ribonucleoprotein [hnRNP] A1, polypyrimidine tract binding protein [PTB] and nucleocapsid protein) or whether it interacts with other viral and

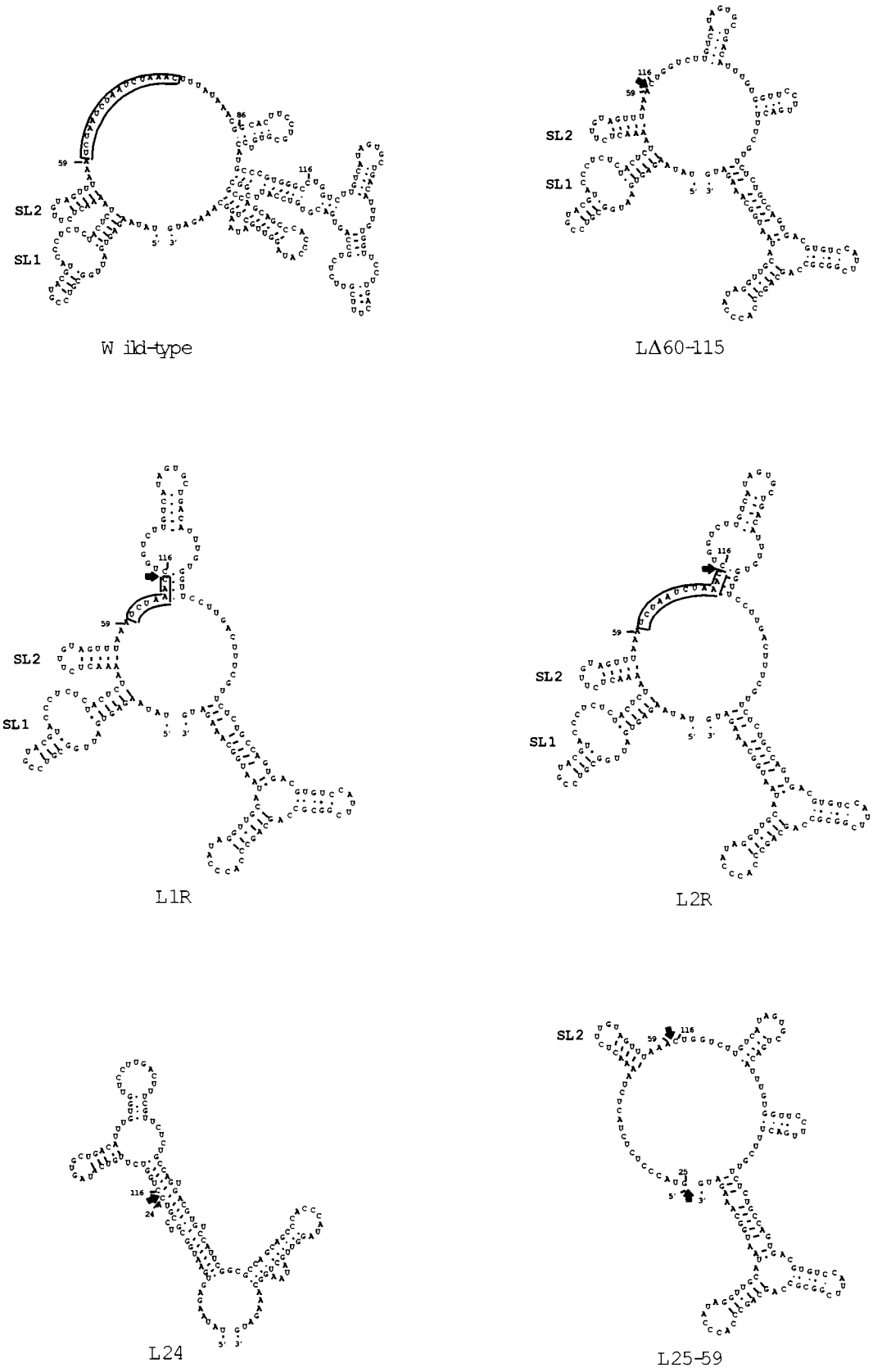

FIG. 6. RNA secondary structure prediction for the 5′-UTR of the wild-type MHV JHM(3) genome and five deletion reporter constructs. The computer program Mfold (45) was used to analyze the secondary structure of the 5′-UTRs of MHV RNA, and the structure was visualized by the software LoopDloop. SL1 and SL2 indicate the two stem-loops at the 5′ end. The consensus repeat sequence in the wild type is boxed. Numbers refer to nucleotide positions in the MHV JHM(3) genome (also see Fig. 1A). Arrows denote the deletion sites in these deletion constructs.

cellular proteins (9, 20, 21, 42). These possibilities are currently under investigation. Alternatively, the 35-nt sequence may serve as an RNA element similar to the DNA enhancer in eukaryotes to enhance the transcription from the downstream promoter (the intergenic sequence in this case) as suggested previously (22). Another possibility is that the 35-nt sequence may provide a structural element to stabilize the transcription complex formed on the leader RNA, allowing more-efficient transcription (see below). It has been shown that the interactions between the 5′-UTR (cloverleaf structure and internal ribosomal entry site) of poliovirus RNA and the cellular poly(rC) binding protein (or hnRNP E) and viral polymerase 3CD regulate poliovirus RNA replication and translation (7). The fourth possibility is that the 35-nt sequence may interact with downstream RNA sequences through pseudoknot interaction. Pseudoknot interaction has been reported for the 3′ region of bovine coronavirus RNA (40). Whether this sequence forms a pseudoknot remains to be determined.

Using computer Mfold (45) and LoopDloop software we have identified that the 5′-end 59-nt sequence forms a stable two-stem-loop structure, while the consensus repeats and the 9-nt sequence are in a single-stranded form (Fig. 6, wild-type). This is in stark contrast to the predicted secondary structure of the leader RNA for equine arteritis virus (39), in which the leader consensus sequence is in a single-stranded loop region at the top of a long stem-loop. Deletions between nt 60 and 135 (see constructs in Fig. 1, 2, and 5) do not disrupt the overall secondary structure of the MHV 5′-UTR region, nor do the 5′-end two-stem-loop structure (Fig. 6, LΔ60-115, L1R, L2R, and further data not shown). These constructs retained the transcription activity (Fig. 2 and 5). When the 5′-end 24 nt is deleted (Fig. 4, construct L25-59), the first stem-loop disappears, while the second stem-loop and the overall secondary structure remain unchanged (Fig. 6, L25-59). The CAT activity expressed from this construct was virtually the same as that from LΔ60-115 (Fig. 4). However, when the sequence between nt 25 and 59 is deleted, the predicted secondary structure changes drastically; both stem-loops no longer exist (Fig. 6, L24). CAT activity expressed from this construct was reduced almost to the background level (Fig. 4). These data suggest that either the overall secondary structure in the 5′-UTR or the second stem-loop or both are important in maintaining a structural requirement that allows transcription to occur. It is thus tempting to suggest that the *cis*-acting enhancer-like function of the sequence between nt 25 and 59 is likely mediated through its role in maintaining the secondary structure. Clearly, further investigations on biochemical mechanisms by which this enhancer-like element exerts in MHV RNA transcription are needed.

Our results show that the 9-nt sequence immediately downstream of the leader up-regulates subgenomic RNA transcription (Fig. 5). This is consistent with our previous findings (42–44). Furthermore, using site-direct mutagenesis, we replaced this 9-nt sequence with a sequence containing the same number of nucleotides and similar RNA secondary structure (data not shown) to determine the effects of space and secondary structure on transcription (Fig. 5). Our result indicates that the regulatory activity appears sequence specific. Thus, this study extends the previous finding on this 9-nt sequence (43, 44). It is noted that the CAT activity of L2R9nt was similar to that of LΔ60-115, which lacks the 9-nt sequence (Fig. 5). If the 9-nt sequence indeed enhances transcription, how does the construct containing the 9 nt have the same level of activity as the one that lacks the 9-nt sequence? A simple interpretation is that the enhancing activity of the 9-nt is possibly counteracted by the inhibitory activity of the two consensus repeats in construct L2R9nt. However, it is intriguing that the construct DECAT-350, which contains three repeats and the 9 nt, exhibited threefold higher CAT activity than those of L2R9nt and LΔ60-115 (Fig. 2B and 5). Arguably, the counterbalance hypothesis does not fully explain this observation. It is possible that the deletion of a sequence between nt 86 and 115 may contribute partially to the lower activity of L2R9nt and LΔ60-115. Secondary structure analysis does not show drastic alteration of the predicted secondary structures for DECAT-350 (identical to the wild-type in Fig. 6) and LΔ60-115. The second stem-loop in L2R9nt is, however, shifted approximately 10 nt downstream, and a downstream single stem-loop forms a double-stem-loop similar to that located downstream of the repeat in constructs L1R and L2R in Fig. 6 (further data not shown). Whether these subtle changes in secondary structure contribute the observed difference in CAT activity in these constructs remains to be seen.

The finding that the consensus repeat sequence possesses a weak inhibitory activity in subgenomic RNA transcription (Fig. 3 and 5) is intriguing. One possible interpretation is that the consensus sequence of the leader may compete with the intergenic consensus sequence or the *trans*-priming leader for the same or different viral and cellular factors, thus resulting in transcription repression. It has been shown recently that hnRNP A1 represses human immunodeficiency virus type 1 pre-mRNA splicing by binding to the exonic splicing silencer sequence of the *tat* exon 2 (4). It will thus be interesting to further investigate the mechanisms by which the consensus sequence of the leader exerts repressive activity. Alternatively, the lower CAT activities observed in DI constructs containing various numbers of the consensus repeat are possibly due to subtle changes in the secondary structure of these deletion mutants as shown in Fig. 6 (compare the stem-loop downstream of the consensus repeat in L1R and L2R with that in the wild-type and LΔ60-115). Alteration of the secondary structure surrounding the consensus repeats in the leader RNA may affect the accessibility of the transcription complex to this region. Nevertheless, the identification of these enhancer-like elements and the characterization of the *cis*-acting sequence in this study should contribute to elucidating the mechanisms by which coronaviruses regulate subgenomic RNA transcription.

ACKNOWLEDGMENTS

This work was supported by Research Project grant RPG-98-090-01-MBC from the American Cancer Society.

We thank Marie Chow for valuable suggestions and discussions throughout this study. We also thank Christopher Lyle for editorial assistance.

REFERENCES

1. **Baker, S. C., and M. M. C. Lai.** 1990. An in vitro system for the leader-primed transcription of coronavirus mRNAs. EMBO J. **9:**4173–4179.
2. **Baric, R. S., and B. Yount.** 2000. Subgenomic negative-strand RNA function during mouse hepatitis virus infection. J. Virol. **74:**4039–4046.
3. **Budzilowicz, C. J., S. P. Wilczynski, and S. R. Weiss.** 1985. Three intergenic regions of coronavirus mouse hepatitis virus strain A59 genome RNA contain a common nucleotide sequence that is homologous to the 3′ end of the viral mRNA leader sequence. J. Virol. **53:**834–840.
4. **Caputi, M., A. Mayeda, A. R. Krainer, and A. M. Zahler.** 1999. HnRNPA/B proteins are required for inhibition of HIV-1 pre-mRNA splicing. EMBO J. **18:**4060–4067.
5. **Chang, R. Y., M. A. Hofmann, P. B. Sethna, and D. A. Brian.** 1994. A *cis*-acting function for the coronavirus leader in defective interfering RNA replication. J. Virol. **68:**8223–8231.
6. **Furuya, T., and M. M. C. Lai.** 1993. Three different cellular proteins bind to complementary sites on the 5′-end-positive and 3′-end-negative strands of mouse hepatitis virus RNA. J. Virol. **67:**7215–7222.
7. **Gamarnik, A. V., and R. Andino.** 1998. Switch from translation to RNA replication in a positive-stranded RNA virus. Genes Dev. **12:**2293–2304.
8. **Hirano, N., K. Fujiwara, S. Hino, and M. Matsumoto.** 1974. Replication and

plaque formation of mouse hepatitis virus (MHV-2) in mouse cell line DBT culture. Arch. Gesamte Virusforsch. **44:**298–302.
9. **Huang, P., and M. M. C. Lai.** 1999. Polypyrimidine tract-binding protein binds to the complementary strand of the mouse hepatitis virus 3′ untranslated region, thereby altering RNA conformation. J. Virol. **73:**9110–9116.
10. **Jeong, Y. S., and S. Makino.** 1994. Evidence for coronavirus discontinuous transcription. J. Virol. **68:**2615–2623.
11. **Kim, Y. N., Y. S. Jeong, and S. Makino.** 1993. Analysis of cis-acting sequences essential for coronavirus defective interfering RNA replication. Virology **197:**53–63.
12. **Kim, Y. N., and S. Makino.** 1995. Characterization of a murine coronavirus defective interfering RNA internal *cis*-acting replication signal. J. Virol. **69:** 4963–4971.
13. **Lai, M. M. C.** 1986. Coronavirus leader-primed transcription: an alternative mechanism to RNA splicing. Bioessays **5:**257–260.
14. **Lai, M. M. C., R. S. Baric, P. R. Brayton, and S. A. Stohlman.** 1984. Characterization of leader RNA sequences on the virion and mRNAs of mouse hepatitis virus, a cytoplasmic RNA virus. Proc. Natl. Acad. Sci. USA **81:**3626–3630.
15. **Lai, M. M. C., P. R. Brayton, R. C. Armen, C. D. Patton, C. Pugh, and S. A. Stohlman.** 1981. Mouse hepatitis virus A59: messenger RNA structure and genetic localization of the sequence divergence from the hepatotropic strain MHV3. J. Virol. **39:**823–834.
16. **Lai, M. M. C., and D. Cavanagh.** 1997. The molecular biology of coronaviruses. Adv. Virus Res. **48:**1–100.
17. **Lai, M. M. C., C. D. Patton, R. S. Baric, and S. A. Stohlman.** 1983. Presence of leader sequences in the mRNA of mouse hepatitis virus. J. Virol. **46:**1027–1033.
18. **Lee, H. J., C. K. Shieh, A. E. Gorbalenya, E. V. Koonin, N. La Monica, J. Tuler, A. Bagdzhadzhyan, and M. M. C. Lai.** 1991. The complete sequence (22 kilobases) of murine coronavirus gene 1 encoding the putative proteases and RNA polymerase. Virology **180:**567–582.
19. **Leibowitz, J. L., K. C. Wilhemsen, and C. W. Bond.** 1981. The virus-specific intracellular RNA species of two murine coronaviruses: MHV-A59 and MHV-JHM. Virology **114:**39–51.
20. **Li, H. P., P. Huang, S. Park, and M. M. C. Lai.** 1999. Polypyrimidine tract-binding protein binds to the leader RNA of mouse hepatitis virus and serves as a regulator of viral transcription. J. Virol. **73:**772–777.
21. **Li, H. P., X. M. Zhang, R. Duncan, L. Comai, and M. M. C. Lai.** 1997. Heterogeneous nuclear ribonucleoprotein A1 binds to the transcription-regulatory region of mouse hepatitis virus RNA. Proc. Natl. Acad. Sci. USA **94:**9544–9549.
22. **Liao, C. L., and M. M. C. Lai.** 1994. Requirement of the 5′-end genomic sequence as an upstream *cis*-acting element for coronavirus subgenomic mRNA transcription. J. Virol. **68:**4727–4737.
23. **Lin, Y. J., and M. M. C. Lai.** 1993. Deletion mapping of a mouse hepatitis virus defective interfering RNA reveals the requirement of an internal and discontiguous sequence for replication. J. Virol. **67:**6110–6118.
24. **Lin, Y. J., C. L. Liao, and M. M. C. Lai.** 1994. Identification of the *cis*-acting signal for minus-strand RNA synthesis of a murine coronavirus: implications for the role of minus-strand RNA in RNA replication and transcription. J. Virol. **68:**8131–8140.
25. **Lin, Y. J., X. M. Zhang, R. C. Wu, and M. M. C. Lai.** 1996. The 3′ untranslated region of coronavirus RNA is required for subgenomic mRNA transcription from a defective interfering RNA. J. Virol. **70:**7236–7240.
26. **Luytjes, W., H. Gerritsma, and W. J. M. Spaan.** 1996. Replication of synthetic defective interfering RNAs derived from coronavirus mouse hepatitis virus-A59. Virology **216:**174–183.
27. **Makino, S., M. Joo, and J. K. Makino.** 1991. A system for study of coronavirus mRNA synthesis: a regulated expressed subgenomic defective interfering RNA results from intergenic site insertion. J. Virol. **65:**6031–6041.
28. **Makino, S., and M. M. C. Lai.** 1989. Evolution of the 5′-end of genomic RNA of murine coronaviruses during passages in vitro. Virology **169:**227–232.
29. **Makino, S., and M. M. C. Lai.** 1989. High-frequency leader sequence switching during coronavirus defective interfering RNA replication. J. Virol. **63:** 5285–5292.
30. **Makino, S., L. H. Soe, C. K. Shieh, and M. M. C. Lai.** 1988. Discontinuous transcription generates heterogeneity at the leader fusion sites of coronavirus mRNAs. J. Virol. **62:**3870–3873.
31. **Makino, S., S. A. Stohlman, and M. M. C. Lai.** 1986. Leader sequences of murine coronavirus mRNAs can be freely reassorted: evidence for the role of free leader RNA in transcription. Proc. Natl. Acad. Sci. USA **83:**4204–4208.
32. **Pachuk, C., P. J. Bredenbeek, P. W. Zoltick, W. J. M. Spaan, and S. R. Weiss.** 1989. Molecular cloning of the gene encoding the putative polymerase of mouse hepatitis coronavirus strain A59. Virology **171:**141–148.
33. **Sawicki, S. G., and D. L. Sawicki.** 1990. Coronavirus transcription: subgenomic mouse hepatitis virus replicative intermediates function in RNA synthesis. J. Virol. **64:**1050–1056.
34. **Sethna, P. B., S. L. Hung, and D. A. Brian.** 1989. Coronavirus subgenomic minus-strand RNAs and the potential for mRNA replicons. Proc. Natl. Acad. Sci. USA **86:**5626–5630.
35. **Shieh, C. K., H. J. Lee, K. Yokomori, N. La Monica, S. Makino, and M. M. C. Lai.** 1989. Identification of a new transcriptional initiation site and the corresponding functional gene 2b in the murine coronavirus RNA genome. J. Virol. **63:**3729–3736.
36. **Spaan, W., H. Delius, M. Skinner, J. Armstrong, P. Rottier, S. Smeekens, B. A. M. van der Zeijst, and S. G. Siddell.** 1983. Coronavirus mRNA synthesis involves fusion of non-contiguous sequences. EMBO J. **2:**1839–1844.
37. **Stohlman, J. A., R. S. Baric, G. N. Nelson, L. H. Soe, L. M. Welter, and R. J. Deans.** 1988. Specific interaction between coronavirus leader RNA and nucleocapsid protein. J. Virol. **62:**4288–4295.
38. **Tahara, S. M., T. A. Dietlin, C. C. Bergmann, G. W. Nelson, S. Kyuwa, R. P. Anthony, and S. A. Stohlman.** 1994. Coronavirus translational regulation: leader affects mRNA efficiency. Virology **202:**621–630.
39. **van Marle, G., J. C. Dobbe, A. P. Gultyaev, W. Luytjes, W. J. M. Spaan, and E. J. Snijder.** 1999. Arterivirus discontinuous mRNA transcription is guided by base pairing between sense and antisense transcription-regulating sequences. Proc. Natl. Acad. Sci. USA **95:**12056–12061.
40. **Williams, G. D., R. Y. Chang, and D. A. Brian.** 1999. A phylogenetically conserved hairpin-type 3′ untranslated region pseudoknot functions in coronavirus RNA replication. J. Virol. **73:**8349–8355.
41. **Zhang, X. M., and M. M. C. Lai.** 1994. Unusual heterogeneity of leader-mRNA fusion in a murine coronavirus: implications for the mechanism of RNA transcription and recombination. J. Virol. **68:**6626–6633.
42. **Zhang, X. M., and M. M. C. Lai.** 1995. Interactions between the cytoplasmic proteins and the intergenic (promoter) sequence of mouse hepatitis virus RNA: correlation with the amounts of subgenomic mRNA transcribed. J. Virol. **69:**1637–1644.
43. **Zhang, X. M., and M. M. C. Lai.** 1996. A 5′-proximal RNA sequence of murine coronavirus as a potential initiation site for genomic-length mRNA transcription. J. Virol. **70:**705–711.
44. **Zhang, X. M., C.-L. Liao, and M. M. C. Lai.** 1994. Coronavirus leader RNA regulates and initiates subgenomic mRNA transcription both in *trans* and in *cis*. J. Virol. **68:**4738–4746.
45. **Zuker, M.** 1989. On finding all suboptimal foldings of an RNA molecule. Science **244:**48–52.